Underwater Acoustic Communication by Passive-Phase Conjugation: Theory and Experimental Results

Daniel Rouseff, *Senior Member, IEEE*, Darrell R. Jackson, Warren L. J. Fox, *Senior Member, IEEE*, Christopher D. Jones, *Member, IEEE*, James A. Ritcey, *Member, IEEE*, and David R. Dowling

***Abstract*—A new method for coherent underwater acoustic communication called passive phase conjugation is evaluated. The method is so named because of conceptual similarities to active phase conjugation methods that have been demonstrated in the ocean. In contrast to active techniques, however, the array in passive phase conjugation needs only receive. The procedure begins with a source transmitting a single probe pulse. After waiting for the multipathed arrivals to clear, the source then transmits the data stream. At each element in the distant receiving array, the received probe is cross-correlated with the received data stream. This cross-correlation is done in parallel at each array element and the results are summed across the array to achieve the final communication signal suitable for demodulation. As the ocean changes, it becomes necessary to break up the data stream and insert new probe pulses. Results from an experiment conducted in Puget Sound near Seattle are reported. Measurements were made at multiple ranges and water depths in range-dependent environments.**

***Index Terms*—Acoustic signal processing, array processing, phase conjugation, underwater acoustic communication.**

I. Introduction

SOUND transmitted in the ocean will often have multiple interactions with the sea surface and the bottom. This multipathing leads to significant time spread as observed at a distant receiver. The pattern of multipath arrivals will change in time as the sea surface evolves, as the properties of the water column change, or as the source moves. It is this combination of multipathing and time variation along with dispersion that makes underwater acoustic communication difficult.

Kilfoyle and Baggeroer recently published a comprehensive review of the state of the art in underwater acoustic communications [1]. Communication systems can be categorized as using either incoherent or coherent modulation strategies. Incoherent processing is based on detecting signal energy where these systems seek to avoid the effects of multipathing by inserting quiescent periods between successive pulses. Essentially, one must wait idly for the duration of the multipath time spread before transmitting the next signal symbol. This approach can be reliable, but not necessarily efficient as much of the time is devoted to waiting for the previous transmission to clear from the sound channel. Coherent processing uses phase detection. These systems can achieve potentially higher data rates because they do not wait for the channel to clear before sending additional symbols. This places the burden on the receiver to correct for the intersymbol interference (ISI) caused by the multipathing. A large body of research has been published on coherent receivers that use adaptive equalization [2] for this task. Typically, there are more than 100 tap delays in the equalizer [3], with [1] quoting an example of successful transmission using 957 taps. These taps must be constantly adjusted to compensate for the changing environment. The resulting computational burden can be substantial. Indeed, in a research context, off-line processing may be required to evaluate the success of a field experiment [4].

In this paper, a new method for coherent underwater acoustic communication called passive phase conjugation is considered. In this approach, an array of receivers is deployed. The spatial diversity provided by the array yields a more complete picture of the multipathing structure and obviates the need for complicated processing at the receiver. Other array-based approaches use beamforming in an attempt to null multipaths [5], but passive phase conjugation exploits multipathing as a natural part of the signal processing. The term "phase conjugation" is used because it can be shown that the processing is related to acoustic time reversal, a subject of active research in the acoustics community [6], [7].

As a method for communication, the proposed procedure is passive in that the array need only receive signals and does not need to transmit. For underwater acoustic communication, the passive phase conjugation procedure should be effective for transmitting information from a remote vessel or vehicle having a single sound source to another vessel or moored installation that has deployed an array of receiving transducers. The procedure begins with transmission of a single probe pulse from the distant sound source and reception of the response at each element of the array. The data stream is then transmitted by the sound source and recorded by each element of the array. The signal processing step involves cross correlating the probe receptions and data streams as observed at an array element. This cross correlation is done in parallel at each array element and the results are summed across the array to achieve the final communication signal ready for demodulation. Compared to adaptive equalization, the procedure is relatively simple and can, in principle, be done in real time. As the ocean changes, it becomes necessary to break up the data stream by inserting new probe pulses.

Manuscript received December 3, 2000; revised July 19, 2001. This work was supported by the Office of Naval Research under Grant N00014-98-G-001.

D. Rouseff, D. R. Jackson, W. L. J. Fox, and C. D. Jones are with the Applied Physics Laboratory, College of Ocean and Fishery Sciences, University of Washington, Seattle, WA 98105 USA.

J. A. Ritcey is with the Department of Electrical Engineering, University of Washington, Seattle, WA 98105 USA.

D. R. Dowling is with the Department of Mechanical Engineering, University of Michigan, Ann Arbor, MI 48109 USA.

Publisher Item Identifier S 0364-9059(01)09161-0.

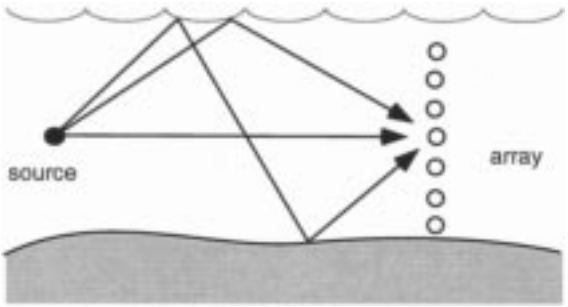

Fig. 1. Experimental configuration for underwater acoustic communication by passive phase conjugation. Multiple acoustic paths between isolated source and distant receive-only array.

Over the last decade, acoustic phase conjugation or time reversal has generated steadily growing interest in the underwater research community. Jackson and Dowling [8] first formulated active phase conjugation for ocean acoustics. In active phase conjugation, the wavefront observed at the array is rebroadcast but in a phase-conjugate (time-reversed) fashion. Dowling [9] studied passive phase conjugation where the array need only receive. Reciprocity was invoked to relate the active and passive techniques. He suggested the method would be useful for pulse compression and acoustic communication. Recently, Silva *et al.* [10] independently proposed a similar passive technique and evaluated it by numerical simulations. Active phase conjugation has been implemented in the ocean [11], [12] and has also been proposed as a method for communication [13], [14]. In this paper, we report first results from a passive phase conjugation experiment conducted in May 2000 near Seattle in Puget Sound.

In Section II, the underlying theory of passive phase conjugation for acoustic communication is outlined. The processing algorithm is evaluated using a normal mode model for the acoustics. Phase shift keying (PSK) is used to encode the data stream. In Section III, results from the experiment are reported. Examples include cases where the source was moored and where it was allowed to drift. The effect of ambient noise is quantified. The utility of embedding new probe pulses in a long data stream is demonstrated.

II. Theory

Fig. 1 shows the basic geometry for underwater communication using passive phase conjugation. The source transmits information to the distant receive-only array. The procedure starts by sending a short probe pulse, waiting for the channel to clear of multipath arrivals, and then sending the data stream.

The passive phase conjugation-signal-processing algorithm is sketched in Fig. 2. The top line shows the probe pulse and subsequent data stream as transmitted by the source. Immediately below are the probe and data stream as observed at each of the M elements in the receiving array. Because of dispersion and multipath propagation, the compact probe pulse is temporally broadened. Similarly, the symbols in the data stream are broadened resulting in ISI from temporal overlap. Because of the spatial diversity, however, each element in the array samples the multipathing structure in a different way. At each element, the observed probe signal is cross-correlated with the data stream. If the probe is a single symbol of the subsequent data stream, this step represents an ideal temporal matched filter that has been automatically calibrated for the signal distortion and spread due to the medium transfer function. The true power in the technique comes from using the spatial diversity provided by the array. The cross-correlations are then coherently summed across the array. The theory of active phase conjugation [8], [11] shows that, if the array samples the multipath structure sufficiently, channel equalization is nearly ideal. Passive phase conjugation [9] approaches this ideal with simpler and less expensive hardware. For communication purposes, the main difference between active and passive implementations is the direction in which the information flows. In the active case, information can be sent from the array to a distant source, while in the passive case the source sends information to the array.

The algorithm suggested in Fig. 2 can be developed more formally. Let the probe symbol be of duration T_s. After propagating through the water column to the receiving array, the pulse broadens to duration T where typically $T \gg T_s$. For an array element located at $\mathbf{r_m}$, denote the measured pressure waveform associated with the probe initiating the sequence as $p_i(\mathbf{r_m}; t)$. After the probe is transmitted, the source is quiet for a temporal guard delay greater than T. The source then sends the data, N consecutive symbols of total duration NT_s. The associated waveform observed at the receiver is $p_d(\mathbf{r_m}; t)$. The cross-correlation between the probe and the data are defined as

$$R_{id}(\mathbf{r_m}; t) = \int_0^T p_d(\mathbf{r_m}; t' + t) p_i(\mathbf{r_m}; t')\, dt'. \tag{1}$$

The output of the processor $S(t)$ is simply the sum of the cross-correlated signals across all M array elements

$$S(t) = \sum_{m=1}^{M} w_m R_{id}(\mathbf{r_m}; t) \tag{2}$$

where the weights w_m have been admitted for generality. The connection with time reversal can be seen in (1) which represents a temporal-filtering operation that is performed with an inversion of the time variable t. Time-domain filtering is usually defined in terms of a convolution where the function to be filtered has the argument $t' - t$, not $t' + t$ as in (1).

To show explicitly how the processor is "phase conjugate," it is necessary to go to the frequency domain. Suppressing the dependence on position, define the Fourier transform pair

$$\tilde{p}(\omega) = \int_{-\infty}^{\infty} p(t) e^{+i\omega t}\, dt$$

$$p(t) = (2\pi)^{-1} \int_{-\infty}^{\infty} \tilde{p}(\omega) e^{-i\omega t}\, d\omega. \tag{3}$$

Combining (1) and (3) and using the fact that the probe is of finite duration it follows that

$$R_{id}(\mathbf{r_m}; t) = (2\pi)^{-1} \int_{-\infty}^{\infty} \tilde{p}_d(\mathbf{r_m}; \omega) \tilde{p}_i^*(\mathbf{r_m}; \omega) e^{-i\omega t}\, d\omega \tag{4}$$

where the fact that $\tilde{p}_i(\mathbf{r_m}; -\omega) = \tilde{p}_i^*(\mathbf{r_m}; \omega)$ for real signals has been exploited. The form of the cross correlation in (4) shows explicitly how the probe signal (or, equivalently, the data stream)

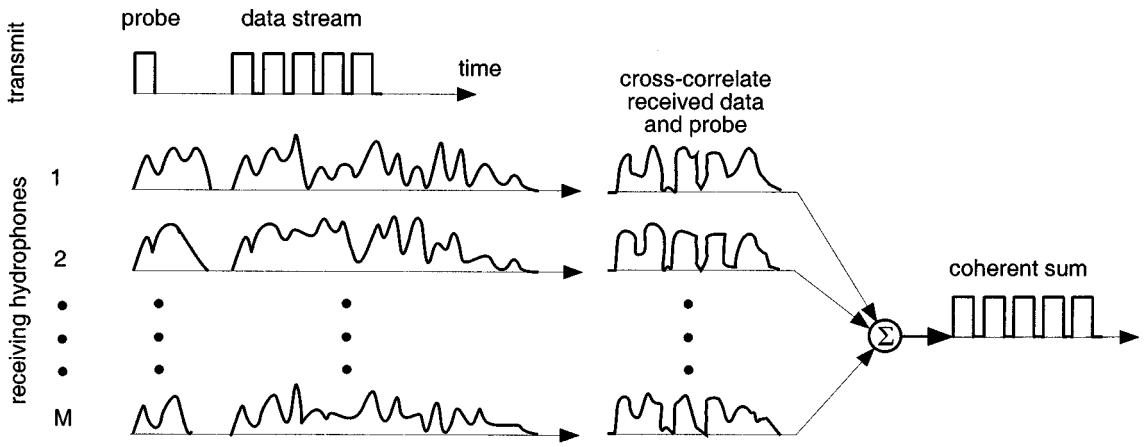

Fig. 2. Passive phase conjugation signal-processing algorithm.

is phase conjugated. In active phase conjugation, it is this step combined with using an active array that allows the backpropagated field to focus at the original location of the source.

One of the strengths of this processing scheme is that it is not tied to any explicit model for the acoustic propagation. To demonstrate that the method reduces ISI, however, it is necessary to choose a particular representation for the acoustic propagation. Consider a modal expansion for the field. While normal modes are more commonly used as a computational tool, they are useful in the present context for their analytical properties. For simplicity, assume that the source and receiving array all lie in the $y = 0$ plane, and that the source lies at $x = 0$ (x is the horizontal range coordinate). The depth of the source is z_0, and the position of the mth element in the receiving array is $\mathbf{r_m} = (x_m, 0, z_m)$. In the frequency domain, the measured field at $\mathbf{r_m}$ due to the data stream is [15]

$$\tilde{p}_d(\mathbf{r_m};\omega) = \tilde{s}_d(\omega) \sum_{\mu} (\xi_\mu x_m)^{-1/2} \Psi_\mu(z_0)\Psi_\mu(z_m) e^{i\xi_\mu x_m}. \tag{5}$$

Here, Ψ_μ is the mode shape, ξ_μ is the associated horizontal wavenumber, and $\tilde{s}_d(\omega)$ is the Fourier transform of the data stream as encoded at the source. For cases with low absorption loss, the modes are real functions of depth and have a weak implicit dependence on frequency. The wavenumbers are complex. Certain unimportant scaling terms in (5) have been suppressed. A similar expression applies for $\tilde{p}_i$, the field from the probe, with $\tilde{s}_i$ being the transformed probe pulse. Substituting these representations into (4) and then (2), it follows that the output, $S(t)$, of the passive phase conjugate processor is

$$S(t) = (2\pi)^{-1} \int_{-\infty}^{\infty} \tilde{s}_d(\omega)\tilde{s}_i^*(\omega)h(\omega)e^{-i\omega t}\, d\omega \tag{6}$$

where the filter

$$h(\omega) = \sum_{\mu}\sum_{\nu} \left(\xi_\mu \xi_\nu^*\right)^{-1/2} \Psi_\mu(z_0)\Psi_\nu(z_0)h_{\mu\nu} \tag{7}$$

and

$$h_{\mu\nu} = \sum_{m=1}^{M} w_m x_m^{-1} \Psi_\mu(z_m)\Psi_\nu(z_m) \exp\left[i\left(\xi_\mu - \xi_\nu^*\right)x_m\right]. \tag{8}$$

The output $S(t)$ involves the desired probe signal and data stream as encoded at the source, but also the additional filter $h(\omega)$. All the complications of the acoustic environment are embedded in this factor. Fortunately, for some special cases, the filter takes a simple form. Consider a well-populated vertical receiving array. The summation in (8) is over the array elements. The weights w_m can be fixed so that the summation approximates an integration in depth. Then by the modal orthogonality condition

$$h_{\mu\nu} \approx \overline{x}^{-1} \exp\left[-2\,\mathrm{Im}(\xi_\mu)\overline{x}\right] \delta_{\mu\nu} \tag{9}$$

where $\overline{x}$ is the common range to each array element and $\delta_{\mu\nu}$ is the Kronecker delta function. The exponential term represents the two-way loss an individual mode would experience in propagating from the source to the array and back. Like its active counterpart, passive phase conjugation cannot correct for loss. Substituting (9) into (7) yields

$$h(\omega) \approx \sum_{\mu} \left(|\xi_\mu|\overline{x}\right)^{-1} \exp\left[-2\,\mathrm{Im}(\xi_\mu)\overline{x}\right] \left|\Psi_\mu(z_0)\right|^2. \tag{10}$$

Note that the filter is a smooth function of frequency without the complicated structure usually associated with multipathing. The exponential acts to attenuate higher order modes and higher frequencies. Note that the modal orthogonality condition has been used in an analogous way to explain active phase conjugation [11]. It is straightforward to generalize the derivation by using a one-way coupled mode acoustic model [16].

Passive phase conjugation works for underwater communication for essentially the same reasons that active phase conjugation works for retrofocusing on remote underwater sound sources [7], [8], [11]. The probe signal provides a full rendering of the acoustic propagation possibilities between the source and the receiving array, and the receiving array exploits this information to combine coherently the signal received on each propagation path. In an underwater sound channel, there are typically several active propagation paths, but the main paths mostly reside near the horizontal so that even a sparse array or an array spanning less than the full water column can often distinguish the paths. In the presence of many propagation paths, the coherent summation across paths significantly reduces the effect of random noise fluctuations.

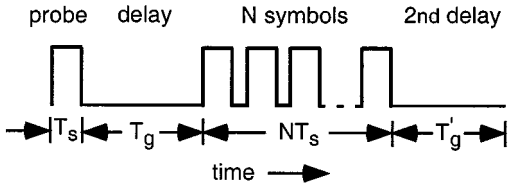

Fig. 3. Telemetry schedule. Data stream broken into N-symbol sections. Schedule is repeated with new probe pulse and next N-symbols until complete data sequence is sent.

In addition, the amplitude weighting of the received signal suppresses noise. The processor weights stronger paths more heavily and suppresses the weak paths thereby emphasizing the higher signal-to-noise portions of a reception.

The main reason that passive phase conjugation works for this application is the pulse compression it provides. This can be deduced from (6) which, for a single positive bit of the data stream, is equivalent to a sum across the array of a convolution of the autocorrelation function of the probe signal and the autocorrelation function of the sound channel's time-dependent Green's function. Both autocorrelation functions will be peaked, so their convolution will be peaked on every channel. The sum across the array then reinforces these peaks and suppresses side lobes (see [9]). The spatial diversity provided by a receiving array is critical here for sidelobe suppression because a single phone can not differentiate between independent signal paths that have nearly the same arrival time. The receiving array is also a very effective means for combating signal fading since simultaneous fading on multiple well-spaced phones is exceedingly unlikely.

The complete communications schedule is represented in Fig. 3. The probe signal takes the form

$$s_i(t) = s(t)\cos(\omega_o t) \tag{11}$$

where ω_o is the carrier frequency and the envelope $s(t)$ is nonzero only in the interval between 0 and T_s. The probe is followed by a guard delay of length T_g and then the N-symbol data stream

$$s_d(t) = \sum_{n=1}^{N} s(t - nT_s - T_g)\cos(\omega_o t + \phi_n). \tag{12}$$

Equation (12) represents a PSK scheme where the information is encoded in the phase ϕ_n. The simplest form is binary PSK (BPSK) where the phase is constrained to be 0 or π and there is one bit per symbol. Higher order schemes allow the phase to take additional values and so increase the number of bits per symbol. Modulation schemes are discussed in Proakis [17] and Simon *et al.* [18].

PSK implemented as part of passive phase conjugation differs from the standard text book applications in some interesting respects. Calculating the Fourier transforms of (11) and (12), and substituting into (6) yields terms proportional to $|\tilde{s}(\omega \pm \omega_o)|^2$. This is the classic response of a matched filter, shifted from baseband to ω_o. Note that if $s(t)$ is of duration T_s, then the output of the matched filter is of duration $2T_s$. This can cause overlap between consecutive symbols in the data stream. The resulting ISI is combated partly in the choice of the envelope $s(t)$ and partly in the design of the receiver. These issues are considered in more detail in the following section. If the ocean environment did not change, there would be no limit to the number of symbols that could be sent before a new probe signal must be sent. In reality, an ocean environment will change and cause the measured data stream to no longer correlate with a once successful, but now obsolete, probe pulse. A similar decorrelation would occur if the location of the source or the array were to change. In practice, these factors impose a limit to the number of consecutive symbols N that can be transmitted. To combat this decorrelation between probe and data, a second guard delay of duration T_g' is inserted after the data stream. One then repeats the telemetry schedule in Fig. 3, sending a fresh probe pulse and an additional N symbols of data whose total time duration does not exceed the environment-imposed correlation time.

The length of the two guard delays, T_g and T_g', and the number of symbols N become crucial design parameters in implementing a communication system based on passive phase onjugation. Excessively long guard delays and small N means a low data rate. Conversely, short guard delays and large N may increase the error rate. As might be expected, the ideal values for these parameters will depend on environmental conditions. These issues are addressed in the following section.

III. Experiment

A passive phase conjugation experiment was performed in Puget Sound near Seattle May 8–12, 2000. Fig. 1 illustrates the basic experiment geometry. The receiving array was deployed from the R/V Henderson in water depths ranging from 30 to 50 m. The source hydrophone was deployed from the R/V Miller at several locations within a 5-km radius of the receiving array in water between 10 and 120 m deep. The R/V Henderson was held in either a two- or three-point mooring, and the array was deployed through the center instrument well of the vessel to minimize array motion. The source was deployed from the stern of the R/V Miller at various locations with the vessel either drifting or moored.

For the cases considered in this paper, the 14-element receiving array was suspended from the R/V Henderson with a clump weight to maintain an approximately vertical alignment of the elements. The array elements were equally spaced and the array spanned the entire water column. The spacing between elements was adjusted depending on the water depth at the deployment site. Each hydrophone (International Transducer Corporation model 6050) in the array has an approximately spherical directivity pattern and a broad operating frequency range. The received signal waveforms on all the hydrophones were simultaneously digitized and recorded onboard the R/V Henderson. The source hydrophone consisted of three broadband cylindrical transducers (International Transducer Corporation model 2044) coupled together in parallel to produce an approximate toroidal point source. The source hydrophones were operated at frequencies of 5–20 kHz with a nominal source level of 192 dB re 1 μPa at 1 m.

The ships were deployed in a shallow water area of Puget Sound at various positions near Spring Beach (47° 44.2′ N, 122° 22.8′ W). Grab samples of the bottom sediment and CTD

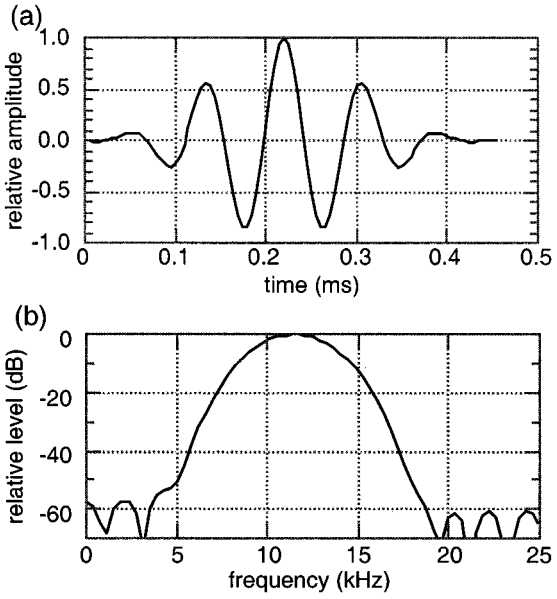

Fig. 4. (a) BPSK symbol. (b) Spectrum of BPSK symbol.

casts were performed to characterize the local environment. The bottom in the general area of operation consisted of a sand/silt sediment. Unless otherwise noted, the bottom topography in the area of operation was generally flat and sloping from the shore. For the cases considered in this paper, the temperature/sound speed profile was nearly constant over the water column with nominal sound speed 1480 m/s. No major oceanographic features were observed. Wind speed and sea state ranged from very calm (sea state 0, wind speed less than 2 m/s) to moderately rough (sea state 2, wind speed 15 m/s). Ambient underwater acoustic noise in the general area was typical for a busy shipping area [19] and ranged from moderately low to high depending on ferry or shipping traffic.

Fig. 4(a) shows the basic BPSK symbol used in the experiment. The pulse was designed by autocorrelating a Hamming windowed 5–18 kHz linear FM pulse. If this symbol represents a "one," then the same symbol but with the opposite sign represents a "zero." The duration is $T_s = 0.460$ ms and since there is only one bit of data per symbol in BPSK, this implies a maximum theoretical data rate of 2.17 kbits/s. Recall that passive phase conjugation uses a probe pulse followed by a guard delay of duration T_g. Because the probe pulse is not part of the data stream, the achievable data rate may approach the theoretical maximum rate but will always be lower. Fig. 4(b) shows the spectrum of the transmitted symbol.

In the remainder of this section, results are presented for various experimental scenarios.

A. Moored Source

For the initial results presented in this subsection, the R/V Miller and R/V Henderson were in two- and three-point moorings, respectively. The distance between vessels was 0.46 km. The source was deployed mid water-column in water 30-m deep. The elements in the receiving array were spaced 2.0 m apart. The sea surface was glassy and there was negligible wind. The moored vessels combined with the benign environment permitted the proposed communications technique to be evaluated under nearly ideal conditions.

The basic symbol shown in Fig. 4(a) was transmitted as the probe pulse, followed by a 50-ms pause, followed by 5 s of data, i.e., 10 869 randomly generated (but known) bits. Fig. 5 shows part of the measured response along each of the 14 elements in the array. Shown is the response due to the probe pulse followed by the start of the data stream. The time spread caused by multipathing is striking; the response to the 0.460-ms probe extends over nearly the entire 50-ms guard delay before the data stream starts.

In this and subsequent runs, it is useful to estimate the signal-to-noise ratio (SNR) in a meaningful way. In passive phase conjugation, multiple arrivals are not regarded as noise that hampers the processing but rather they are treated as useful signal. To estimate the effective SNR, ambient noise energy was calculated at each receiving element for the 50 ms prior to the first arriving signal. The energy was then calculated for the 50 ms beginning with the first arrival. This contains both signal energy (including both the direct path and the multipaths) and the noise. The difference between the two calculations is an estimate of the signal energy. The signal energy, averaged across the hydrophones, compared to the average noise gives the effective SNR. For the example in Fig. 5, SNR $= 24.1$ dB.

The gain introduced by passive phase conjugation is also demonstrated in Fig. 6. The response at each hydrophone due to the probe pulse only in Fig. 5 is autocorrelated, giving the effective result of a single symbol of the communication stream in isolation. The thin line in Fig. 6 shows the average energy level in these autocorrelated probe signals obtained by averaging the magnitude squared of the complex envelopes (i.e., incoherently averaging the autocorrelated responses across the array), and converting to dB. There is a sharp central peak, but also significant side lobe structure. The side lobes are a consequence of the responses from the different acoustic paths, visible for each waveform in Fig. 5, correlating with one another. Since each hydrophone samples a different multipath structure, each will have different side lobes. By taking the coherent sum across the array elements, as is done in passive phase conjugation, the contribution from the side lobes is effectively reduced relative to the central peak. This is shown in the thick line in Fig. 6, which is the magnitude squared of the complex envelope of the coherently averaged time series in decibels. Reducing the side lobes reduces the ISI and hence improves communication robustness. For independent multipath structures on each hydrophone, the theoretical processing gain is $10\log(M)$ dB, where M is the number of elements in the array. In this case, $M = 14$ resulting in a theoretical gain of roughly 11.5 dB, which is consistent with Fig. 6.

The probe pulses shown in Fig. 5 were cross-correlated with the subsequent data as in (1). Adding the cross-correlated signals yielded the output of the processor, denoted as $S(t)$ in (2). Differential PSK (DPSK) was used to modulate the data stream. To demodulate the measured $S(t)$, it is first multiplied by a time delayed version of itself, $S(t - T_s)$, and the product is then integrated over intervals of duration T_s. The result is a sequence of real numbers. In effect, differences in phase between a successive pair of symbols are translated into a real

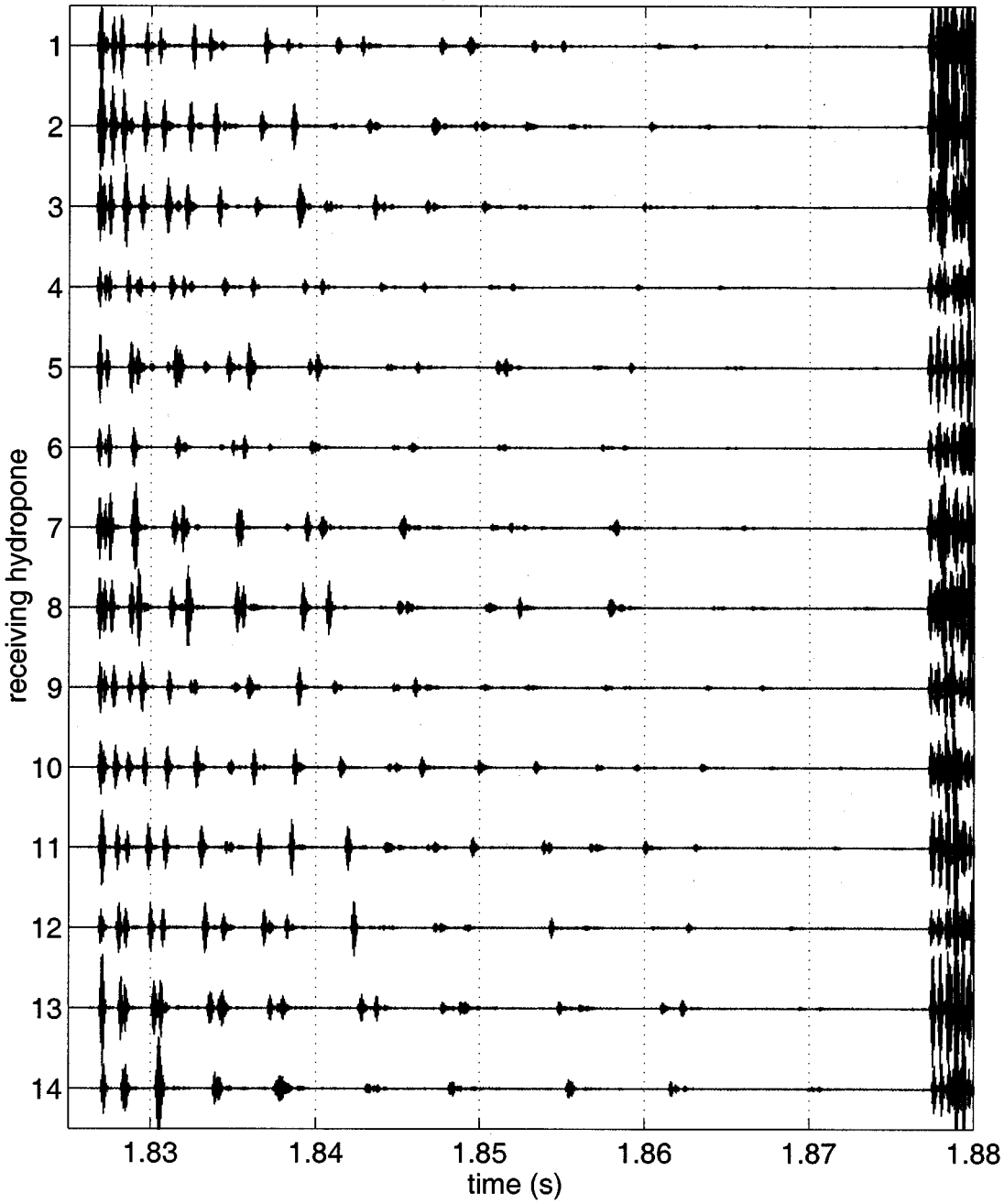

Fig. 5. Response along each element in receiving array from transmitted probe pulse. Also shown is beginning of response to data stream transmitted $T_g = 50$ ms later. Top time series is for shallowest array element.

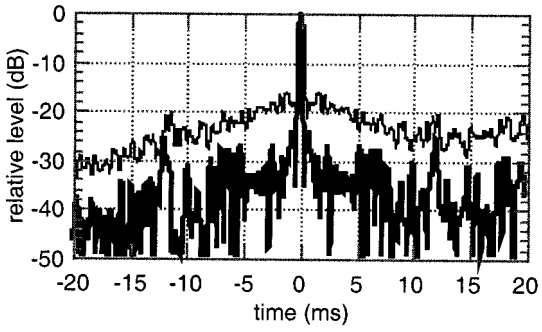

Fig. 6. Autocorrelation of probe pulse. Thin line is incoherent average across the array; dark line is coherent average. Coherent averaging reduces side lobes.

number [20]. As implemented, a positive value is interpreted as a transmitted "one" while a negative value corresponds to a "zero." If the number is close to zero, the results are ambiguous and the probability of bit error is higher. Fig. 7 is a scatter plot showing the demodulated output plotted as a function of time. A transmitted "one" is plotted as an "x" while a circle denotes a transmitted "zero." Initially, the positive and negative clusters in Fig. 7 are widely separated. The distance between the clusters decreases, but stabilizes after about 0.5 s. The two clusters remain separated and the communication is, in fact, error free; each "x" lies above the zero line while each circle lies below it. For the present scenario, the environment is sufficiently benign that a five-second-old probe pulse can still be used to recover a

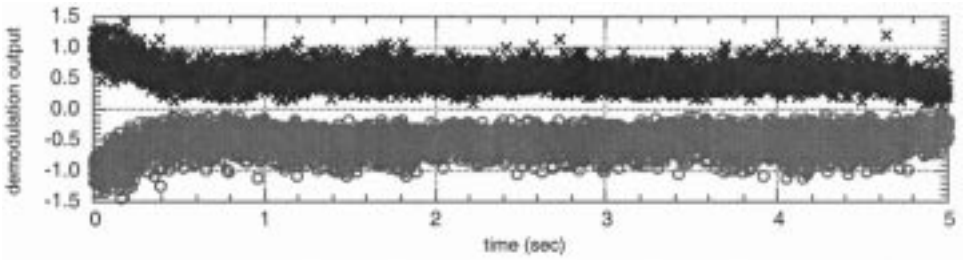

Fig. 7. Demodulation output, benign conditions. Dark "x" indicates transmitted "one," shaded circle indicates transmitted "zero." Range to receiving array is 0.46 km, SNR as defined in text is 24.1 dB. Clusters of symbols are isolated from each other and communication is error free at 2.15 kbits/s.

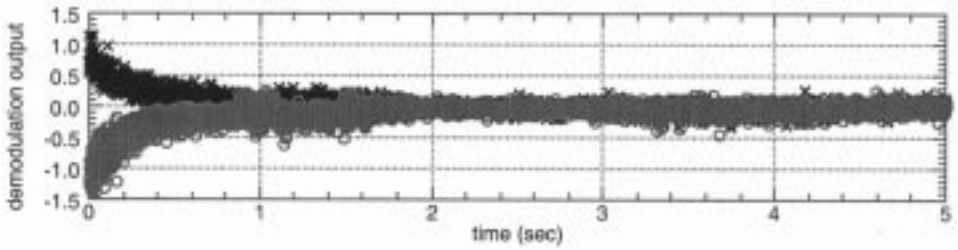

Fig. 8. Demodulation output, windy conditions. Range to receiving array is 0.92 km, SNR = 8.1 dB. Communication is error free for 0.474 27 s (1032 symbols) before two clusters begin to merge.

data stream even in the presence of the multipathing implied by Fig. 5. The data rate is less than the theoretical maximum only because of the short time, $T_s + T_g = 50.46$ ms, necessary to send the probe pulse and wait for the channel to clear.

Fig. 8 shows an example of the demodulation output determined under less benign environmental conditions. The R/V Miller and R/V Henderson were in one- and two-point moors, respectively, with the range increased to 0.92 km. The wind speed was 8 m/s and breaking waves were observed. The estimated SNR decreased to 8.1 dB. The first bit error in Fig. 8 occurs at 0.474 27 s, and shortly thereafter the two clusters merge. In such an environment, successful communication would require breaking long data sequences into approximately 1000-bit sections and inserting new probe pulses.

For the cases shown in Figs. 7 and 8, the nominal water depth was 30 m with only mild changes in bathymetry between the source and the receiving array. In order to test the method in a strongly range-dependent environment, the source was moved so that the propagation path straddled a 78-m deep cavity. Fig. 9(a) shows the bathymetry where the range between the source and receiver is 1.6 km. Superimposed on the figure is a ray trace. Shown are rays leaving the source at launch angles between $\pm 30^\circ$ with 1.5° spacing. Rays hitting the far end of the cavity are made steeper thereby reducing the cycle distance between bottom interactions. A ray is removed from the calculation after six bounces off of the bottom. Examination of the measured response along the receiving array (not shown) reveals a dense structure of multipaths arriving over a relatively short time. The late arrivals effectively blend into the noise after 20 ms. This should be compared to Fig. 5 where late arrivals are still being detected up to 50 ms after the first arrival. A shorter effective time spread should reduce the ISI between transmitted symbols widely separated in time. Fig. 9(b) is a scatter plot of the measured demodulation output for this case. The two clusters are widely separated over the entire 5-s window and the communication is error free.

B. Drifting Source

In another suite of measurements, the R/V Miller was allowed to drift as it transmitted. This increases the source motion and is more representative of an acoustic communications scenario with a slowly moving ROV. The R/V Henderson was in a two-point moor in 30-m deep water. The array spacing was 2.0 m.

Fig. 10 shows the scatter plots for several transmission sequences. In all cases, a single probe pulse was followed by a 50-ms guard delay and a 5-s long telemetry stream. In Fig. 10(a), the water depth at the R/V Miller is 60 m and the range to the receiving array is 1.5 km. Occasional wave breaking was observed and the wind speed was 5 m/s. The calculated SNR was 11.8 dB. The two clusters are well separated and the communication is error free. Fig. 10(b) shows results measured 36 min later. The R/V Miller was repositioned to range 2.5 km at depth 96 m, and again allowed to drift. The wind had increased to 7 m/s with higher gusts and the SNR was reduced to 5.5 dB. The two clusters remain separated for 2.5 s before they merge. Fig. 10(c) shows results measured 86 s later. The SNR had improved to 9.3 dB. In this case, the two clusters remain separated for the entire 5 s.

These results for a drifting source can be understood by considering the size of the retrofocus of an active time reversing array in the same environment. Neglecting for the moment ocean surface dynamics and array motion, the size of the retrofocus region for the active case is set by the frequency content of the signal and the characteristics of the waveguide. For passive phase conjugation, the probe's retrofocus region is the region of space where the correlation of array-received probe signals from the same source at different locations would

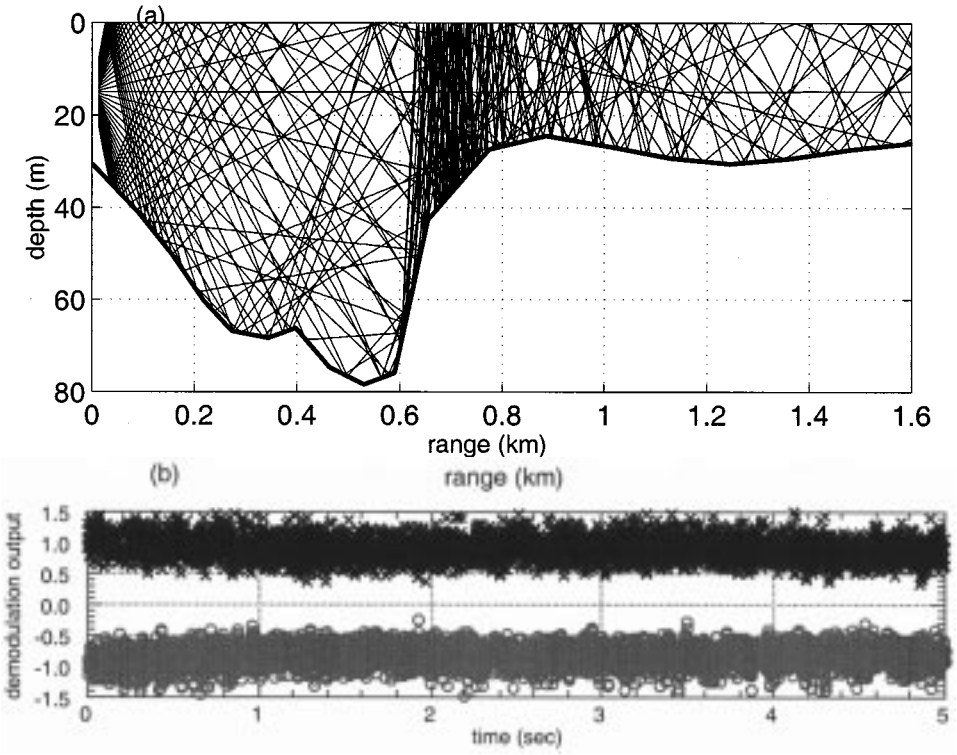

Fig. 9. Communication over varying bathymetry. (a) Bathymetry and ray trace. (b) Demodulation output, SNR = 8.1 dB.

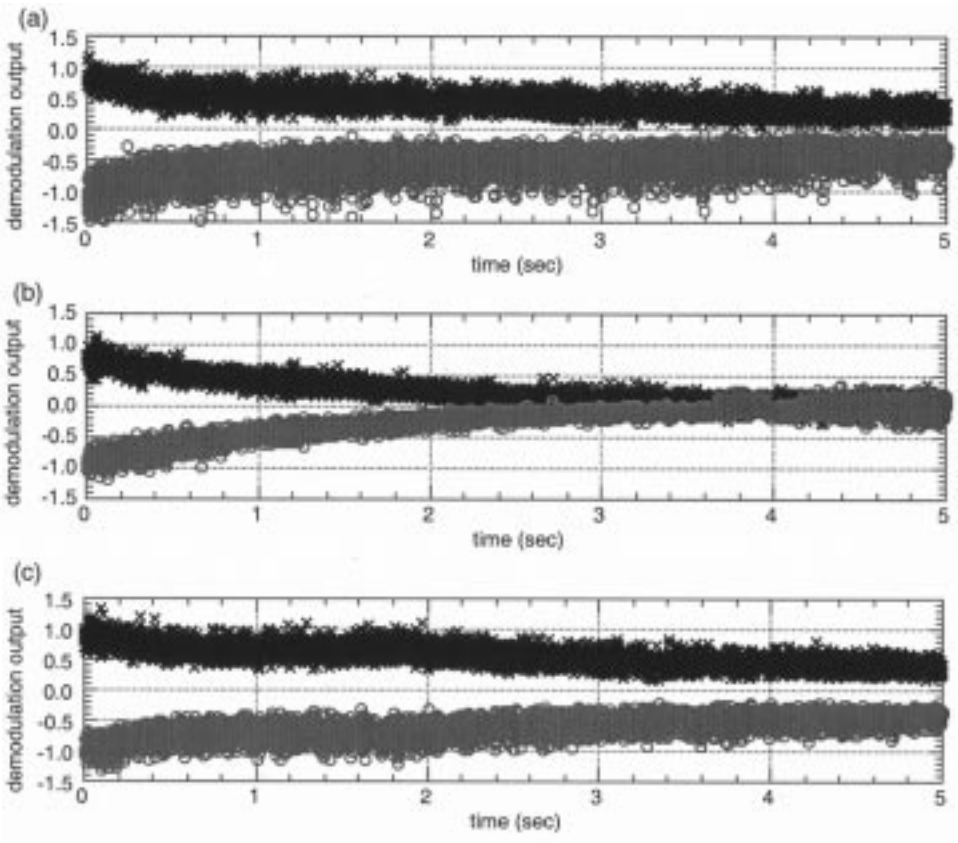

Fig. 10. Demodulation output for drifting source scenario. (a) Range 1.5 km, drift rate 0.4 m/s, SNR = 11.8 dB. (b) Range 2.5 km, drift rate 0.5 m/s, SNR = 5.5 dB. (c) Range 2.5 km, drift rate 0.5 m/s, SNR = 9.3 dB, measurement made 86 s after previous case. See text for details.

be high. In underwater waveguides, such active or passive retrofocus regions are typically elongated in the source-array and cross-range directions compared to the depth direction [11], [21]. Consequently, passive phase conjugation-based

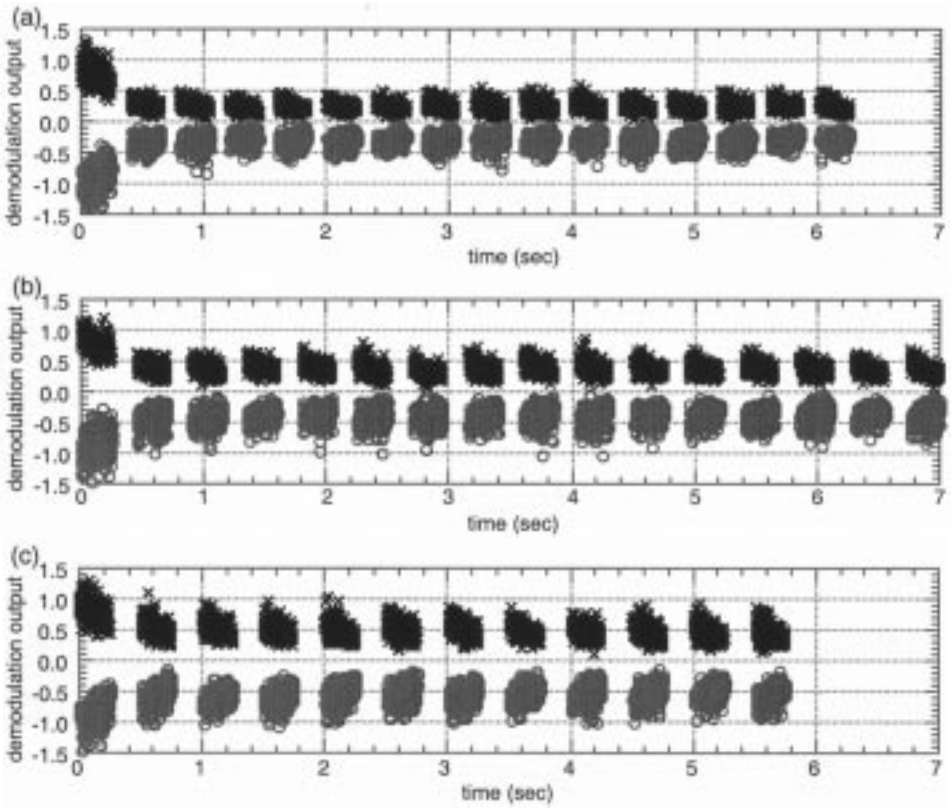

Fig. 11. Segmented data stream. Length of guard delay T_g' varied after 250 ms segment of data. (a) $T_g' = 100$ ms, SNR = 10.9 DB. (b) $T_g' = 150$ ms, SNR = 11.2 dB. (c) $T_g' = 200$ ms, SNR = 12.7 dB. See text for details.

TABLE I
SUMMARY OF FIG. 11 RESULTS. MEAN MAGNITUDE OF DEMODULATION OUTPUT WITH STANDARD DEVIATION, DATA RATE, AND ERROR RATE

T_g' (msec)	demodulation output	data rate (kbits/s)	error rate
100	0.275±0.094	1.38	2.3×10^{-4}
150	0.383±0.120	1.23	0
200	0.517±0.142	1.12	0

communication systems may be effective as long as the drifting source stays at the same depth and does not move beyond the retrofocus region defined by the most recent probe transmission. Obviously, reprobing is necessary once the source's drift distance exceeds the probe's retrofocus size. A simple calculation is instructive: assuming a 0.5 m/s drift rate, a center frequency of 15 kHz and a nominal sound speed of 1500 m/s, over the course of 5 s a drifting source would move 25 wavelengths. The successful results in Fig. 9 demonstrate that source motion at these scales does not destroy the communication process. For the cases shown, the factor limiting successful communication appears to be changes in the environment rather than excessive source drift.

C. Segmented Data Stream

Eventually, a measured probe response no longer correlates with a measured data stream. This might be because of source and/or receiver motion, or because the propagation environment changes. A relatively low SNR might exaggerate the problem. To send data sequences that are longer than the acoustic decorrelation time, it is necessary to break up the data stream into shorter segments and intersperse new probe pulses. For measurements reported in this section, the data were broken into 543-bit sequences so $NT_s = 250$ ms. This is a conservative choice relative to the decorrelation time observed in the previous sections. After each data sequence, a guard delay of duration T_g' (Fig. 3) is introduced, followed by a new probe pulse, another guard delay $T_g = 50$ ms, and additional data.

For the results reported in this section, both the R/V Miller and R/V Henderson were moored. The range was 0.65 km and the water depth was 30 m. The receiving array was deployed with 1.7-m spacing between the elements. The wind speed was 6 m/s and the water column remained nearly isovelocity.

Fig. 11 shows the demodulation output for various values of T_g', the guard delay after a data segment. Consider Fig. 11(a) where $T_g' = 100$ ms. The two clusters are well separated for the first data segment, time less than 250 ms. The clusters for subsequent data segments, however, are closer together. While generally still separated, some symbols are ambiguous; there are, in fact, two bits that are incorrectly demodulated. The situation improves in Fig. 11(b) where $T_g' = 150$ ms the later data segments are more widely separated than in Fig. 11(a). There are no

bit errors in this case. Finally, in Fig. 11(c) the guard delay has been increased to $T_g' = 200$ ms. The subsequent data clusters are nearly as well separated as the first and the communication is error free.

Results for the three cases shown in Fig. 11 are summarized in Table I. The mean value of the magnitude of the demodulation output is tabulated with the associated standard deviation. (To remove bias and better compare the results for different values of T_g', the first data segment, time less than 250 ms, have been excluded from the calculations.) The magnitude of the demodulation output increases with increased guard delay T_g'. Also tabulated are the data and error rates. Increasing T_g' increases the accuracy at the cost of a small decrease in efficiency.

The separation between the clusters in Fig. 11 increases with T_g' and the communication becomes more reliable. The observation that the delay after a data segment needs to be larger than the delay after a probe pulse can be understood as follows. The energy in a received probe seems to die out after a relatively short time, 50 ms in the example shown in Fig. 5. In reality, a small amount of energy remains. These late-arriving paths are buried in the ambient noise and not observable when the probe is transmitted alone. However, when hundreds of data symbols are transmitted back-to-back, the late arrivals can add and produce an energy level above the ambient noise. This late-arriving energy can corrupt the next probe signal when T_g' is too small. Consequently, it is necessary to wait longer for the channel to clear completely after a long data sequence.

IV. Concluding Remarks

Experimental results have been presented demonstrating the passive phase conjugation method for underwater acoustic communication. The method uses an array of receiving hydrophones. In contrast to active phase conjugation, the array needs only receive and not also transmit. The method makes use of a measured probe pulse to characterize the acoustic environment and thereby exploit multipath propagation. As the ocean changes, it becomes necessary to re-estimate the channel impulse response for each of the receiving hydrophones. The simplest method for getting new estimates, and the one pursued in this paper, is to break-up a long data stream and insert new probe pulses.

One of the strengths of passive phase conjugation is its computational simplicity. Coherent communication methods based on adaptive equalizers, by contrast, often have a significant computational burden. The number of tap delays is typically on the order of 100 or more, and the weights for these delay lines must be constantly adjusted. The adjustments required in passive phase conjugation are less frequent and can be accomplished by simply transmitting a new probe pulse. A hybrid system could likely be developed where the output of the passive phase conjugation processor is fed into an equalizer. This might correct for residual ISI or Doppler effects. The goal would be to develop an equalizer with a much-reduced number of taps.

The length of time needed to clear the channel for an acceptable error level depends on range, signal type, number of symbols, length of transmission, ambient noise, and environmental conditions. Further investigation will produce guidelines for the number of symbols that can be sent before reprobing and the length of the guard delay before another data segment can be transmitted under various environmental conditions. We will also investigate issues regarding data rate and computational complexity when the channel impulse response is discerned by continuous adaptive estimation rather than reprobing.

References

[1] D. B. Kilfoyle and A. B. Baggeroer, "The state of the art in underwater acoustic telemetry," *IEEE J. Oceanic Eng.*, vol. 25, pp. 4–27, Jan. 2000.

[2] M. Stojanovic, J. A. Catipovic, and J. G. Proakis, "Phase-coherent digital communications for underwater acoustic channels," *IEEE J. Oceanic. Eng.*, vol. 19, pp. 100–111, Jan. 1994.

[3] M. Stojanovic, "Recent advances in high-speed underwater acoustic communication," *IEEE J. Oceanic Eng.*, vol. 21, pp. 125–136, Apr. 1996.

[4] E. Bovio, "A review of the applicability of UUV technology to mine countermeasures," NATO SACLANT Undersea Res. Centre, La Spezia, Italy, SM-345, 1999.

[5] L. R. LeBlanc and P.-P. J. Beaujean, "Spatio-temporal processing of coherent acoustic communication data in shallow water," *IEEE J. Oceanic Eng.*, vol. 25, pp. 40–51, Jan. 2000.

[6] M. Fink, "Time-reversed acoustics," *Phys. Today*, vol. 50, no. 3, pp. 34–40, 1997.

[7] ——, "Time-reversed acoustics," *Sci. Amer.*, vol. 281, no. 5, pp. 91–97, 1999.

[8] D. R. Jackson and D. R. Dowling, "Phase conjugation in underwater acoustics," *J. Acoust. Soc. Amer.*, vol. 89, no. 1, pp. 171–181, 1991.

[9] D. R. Dowling, "Acoustic pulse-compression using passive phase-conjugate processing," *J. Acoust. Soc. Amer.*, vol. 95, no. 3, pp. 1450–1458, 1994.

[10] A. Silva, S. Jesus, J. Gomes, and V. Barroso, "Underwater acoustic communication using a 'virtual' electronic time-reversal mirror approach," in *Proceedings of the fifth European Conference on Underwater Acoustics*, M. E. Zakharia, Ed. Luxembourg, Luxembourg: European Commission, 2000, pp. 531–536.

[11] W. A. Kuperman, W. S. Hodgkiss, H. C. Song, T. Akal, C. Ferla, and D. R. Jackson, "Phase conjugation in the ocean: Experimental demonstration of an acoustic time-reversal mirror," *J. Acoust. Soc. Amer.*, vol. 103, no. 1, pp. 25–40, 1998.

[12] W. S. Hodgkiss, H. C. Song, W. A. Kuperman, T. Akal, C. Ferla, and D. R. Jackson, "A long-range and variable focus phase-conjugation experiment in shallow water," *J. Acoust. Soc. Amer.*, vol. 105, no. 3, pp. 1507–1604, 1999.

[13] A. A. M. Abrantes, "Examination of time-reversal acoustics in shallow water and applications to underwater communications," M.S. thesis, Naval Postgraduate School, Monterey, CA, 1999.

[14] T. Akal, G. Edelmann, S. Kim, W. S. Hodgkiss, W. A. Kuperman, and H. C. Song, "Low and high frequency ocean acoustic phase conjugation experiments," in *Proceedings of the fifth European Conference on Underwater Acoustics*, M. E. Zakharia, Ed. Luxembourg, Luxembourg: European Commission, 2000, pp. 989–994.

[15] F. B. Jensen, "Wave theory modeling: A convenient approach to CW and pulse propagation modeling in low-frequency acoustics," *IEEE J. Oceanic Eng.*, vol. 13, pp. 186–197, Oct. 1988.

[16] M. Siderius, D. R. Jackson, D. Rouseff, and R. P. Porter, "Multipath compensation in shallow water environments using a virtual receiver," *J. Acoust. Soc. Amer.*, vol. 102, pp. 3439–3449, 1997.

[17] J. G. Proakis, *Digital Communications*. New York: McGraw Hill, 1995.

[18] M. K. Simon, S. M. Hinedi, and W. C. Lindsey, *Digital Communication Techniques*. Englewood Cliffs, NJ: Prentic- Hall, 1995.

[19] R. J. Urick, *Principles of Underwater Sound*, 3rd ed. New York: McGraw Hill, 1983, p. 212.

[20] A. B. Carlson, *Communications Systems*, 3rd ed. New York: McGraw Hill, 1986, pp. 539–541.

[21] M. R. Dungan and D. R. Dowling, "Computed narrow-band time-reversing array retrofocusing in a dynamic shallow ocean," *J. Acoust. Soc. Amer.*, vol. 107, no. 6, pp. 3101–3112, 2000.

Daniel Rouseff (S'86–M'89–SM'95) received the Ph.D. degree in electrical engineering from the University of Washington, Seattle, in 1989.

After graduation, he joined the senior professional staff at the Milton S. Eisenhower Research Center of The Johns Hopkins University Applied Physics Laboratory, Laurel, MD. He joined the University of Washington in 1992, where he is currently a Senior Engineer at the Applied Physics Laboratory. During the summer of 1997, he was an A.S.E.E.-U. S. Navy Senior Faculty Fellow at the Naval Research Laboratory, Washington, DC. In 2001, he was a Senior Visiting Fellow in the Department of Applied Mathematics and Theoretical Physics at the University of Cambridge, Cambridge, MA. His primary technical interests are ocean acoustics and tomography.

Dr. Rouseff is a member of the Acoustical Society of America and the scientific advisory board for the International Acoustical Imaging Symposia.

Darrell R. Jackson received the B.S. and Ph.D. degrees from the University of Washington, Seattle, in 1960, and 1966, respectively, both in electrical engineering, and the Ph.D. degree in physics from the California Institute of Technology, Pasadena, in 1977.

From 1960 to 1967, he worked at the Boeing Company as a Research Engineer. He joined the Electrical Engineering faculty of the University of Massachusetts, Amherst, in 1968 and returned to graduate school in 1972. Since 1976, he has been with the Applied Physics Laboratory of the University of Washington, where his research is centered on acoustical oceanography and underwater acoustics with emphasis on acoustic interaction with the seafloor.

Dr. Jackson is a Fellow of the Acoustical Society of America and a member of the American Geophysical Union.

Warren L. J. Fox (M'89–SM'01) received B.S.E.E., M.S.E.E., and Ph.D. degrees in electrical engineering from the University of Washington, Seattle, in 1988, 1990, and 1994, respectively.

From 1988 through 1995 he was a professional staff member at the Applied Physics Laboratory, University of Washington (APL-UW). From 1996 to 1998, he was a Scientist with the NATO SACLANT Undersea Research Centre, La Spezia, Italy. He rejoined APL-UW in 1999, and became an Affiliate Assistant Professor in the Department of Electrical Engineering in 2000. His research projects involve environmentally adaptive sonar control and underwater acoustic communications. His research interests span a wide range of topics involving theoretical/applied ocean acoustics and statistical signal processing.

Christopher D. Jones (M'99) received the B.S. and M.S. degrees in mechanical engineering from the University of Massachusetts, Amherst, in 1985 and 1987, respectively, and the Ph.D. degree in electrical engineering from the University of Washington, Seattle, in 1999, specializing in acoustic and electromagnetic wave propagation and scattering.

From 1987 to 1994, he worked as a Research Engineer in the Acoustics Division and the Marine GeoSciences Division of the Naval Research Laboratory, Washington, DC. He is currently a member of the Ocean Acoustics Department at the Applied Physics Laboratory of the University of Washington, Seattle. His present research interests include acoustic remote sensing in the ocean, wave propagation and scattering in random media, and numerical modeling of acoustic wave scattering at the seafloor.

Dr. Jones is a member of the Acoustical Society of America.

James A. Ritcey (M'76) received the B.S.E. degree from Duke University, Durham, NC, the M.S.E.E. degree from Syracuse University, Syracuse, NY, and the Ph.D. degree in electrical engineering (communication theory and systems) from the University of California, San Diego, in 1985.

Since 1985, he has been with the Department of Electrical Engineering at the University of Washington, Seattle, where he now holds the rank of Professor. From 1976 to 1981 he was with the General Electric Company, and graduated from GE's Advanced Course in Engineering. His research interests include communications and statistical signal processing for radar, underwater acoustics, and biomedicine. He has published over 100 papers in these areas.

Prof. Ritcey served as the General Chair of the 1995 International Conference on Communications in Seattle. He also served as Technical Program Chair of the 1992 and General Chair of the 1994 Asilomar Conference on Signals, Systems, and Computers and is currently a member of the Steering Committee.

David R. Dowling received the Ph.D. degree in aeronautics from the California Institute of Technology, Pasasena, in 1988.

He worked at Boeing Aerospace for a year before taking a post-doctoral position at the Applied Physics Laboratory of the University of Washington. In 1992, he accepted an assistant professor position in the Department of Mechanical Engineering at the University of Michigan and was promoted to associate professor in 1999. His current research interests include photoacoustics, underwater sound, hydroacoustics, and turbulence.

Dr. Dowling is a member of the Acoustical Society of America, the American Physical Society, and the American Society of Mechanical Engineers.